

Referee 1

(1) In the Introduction on p. 455 (lines 22-26), it is noted that Portmann et al. (2012) showed that an increase in N₂O emission at the surface would lead to a global mean decrease in ozone in the 30-35 km region. This seems to be inconsistent with the mechanisms discussed in the rest of the paper. For example, in the next sentence it is noted that Plummer et al. find that an increase in global N₂O at 10 hPa leads to an ozone increase there. So, please provide an explanation here or later in the paper.

This was indeed confusing. We have rewritten this as:

Plummer et al. [2010] studied O₃ changes in a model including GHGs and ODSs. They ran two experiments with a faster Brewer-Dobson circulation, and these two experiments showed, at 10 hPa in the tropics, a decrease in reactive nitrogen and an increase in both O₃ and N₂O at 10 hPa relative to the experiments with a slower circulation. Thus variations in O₃ and N₂O at 10 hPa can be either correlated or anti-correlated depending upon whether they are driven by circulation or by changes in N₂O entering the stratosphere.

(2) P. 456, lines 23-27. Here some key results of the analysis are stated in the Introduction. Normally, it is better to state only what will be done and why in the Introduction and save the results for later. Probably the purpose is to motivate the reader to read the full paper, but this can usually be done without giving away the results. Just an optional suggestion.

The reviewer may have a point; however, we felt that it would be useful to give a roadmap where we were headed before going into details.

(3) P. 458, line 20. "Lasp"?

LASP is Laboratory for Atmospheric and Space Physics. The text has been corrected.

(4) P. 464, line 20. "doubled to 1 km"? Does this mean that the resolution was 0.5 km and was changed to 1 km? Please make this clear.

This now reads: "Compared with those earlier studies, the present model has an improved vertical resolution (1 km instead of 2 km)."

(5) P. 464-466, Model calculations and summary. Use of the CHEM2D model, as done in this manuscript, is a logical first step toward understanding the dynamical and chemical processes that apparently lead to the observed negative O₃ trends in the tropical middle stratosphere over the 1991-2014 period. However, to verify these results and investigate other aspects of ozone trends (such as the ozone increase in the SH midstratosphere seen by MLS), 3D models with interactive chemistry and coupled oceans are probably needed. A suggestion for future work is to consider analyzing CMIP-5 model results (Taylor et al., BAMS, v. 93, p. 485, 2012). A number of the CMIP-5 models included interactive ozone chemistry and coupled oceans. The historical simulations were intended to account for known anthropogenic and natural forcings and extended from the mid-1800's to 2005, which overlaps significantly with the period studied in this manuscript. The model data are archived so it is straightforward to analyze the data and investigate whether the SH positive O₃ trend, for example, is simulated

by any of these models.

This certainly does sound like a good idea for future work. It would certainly be interesting to see how the 10 hPa tropical ozone responds to a variety of forcings. We have added a sentence in the summary suggesting this.

There is no Referee 2

Referee 3

This paper utilizes satellite measurements to show evidence for a decrease in tropical ozone near 30 km since 1991, and proposes a relatively simple explanation due to changes in circulation and reactive nitrogen. This is a novel and interesting paper. The results show straight-forward analyses of ozone measurements from HALOE (1991-2005) and MLS satellites (2004-2013), which highlight the middle stratosphere ozone decreases; the authors note similar results in other recent observational studies. The proposed mechanism for ozone decreases involves an increase in reactive nitrogen (NO_y), linked to decreases in N₂O (possibly related to a decreased tropical upwelling circulation). The evidence for this mechanism is: 1) positively coupled ozone – N₂O from MLS data, (2) consistent changes in ozone – N₂O – NO_y from ACE-FTS measurements, (3) observed trends in ozone and NO_x from HALOE, and (4) results from an idealized chemical transport model with imposed circulation changes (which explains the altitude dependence and approximate magnitude of ozone – NO_y changes). All of this evidence is consistent with the hypothesis of variations in NO_y causing the observed ozone decrease, and overall a convincing case is made. This paper is appropriate for ACP, and makes an important contribution to understanding long-term ozone variability. Overall the paper is well written and clear, although I have a few comments for the authors to consider in revision.

1) The authors might include a reference to Bourassa et al (ACP, 2014), who derive a similar ozone decrease in the tropics from combined SAGE II – OSIRIS data.

A brief description of this reference has been added to the introduction.

2) I think it would be useful to include a figure showing the latitude-height structure of linear trends in MLS N₂O measurements, to complement the ozone trends (Fig. 3) and bolster the arguments regarding links in ozone – N₂O trends. Note that the strong correlations in Figs. 4-6 could mainly reflect QBO variations (which appear to dominate in Fig. 5).

Indeed, the strong correlations in Figures 4-6 almost certainly do, to a large extent, reflect QBO variations. Hence Figure 7 is quite important. A figure showing the N₂O trends is actually already in Atmos. Chem. Phys. Discuss., 15, 1–27, 2015.

3) I like the arguments regarding estimated sensitivities of $\Delta(\text{ozone}) / \Delta(\text{NO}_y)$ in lines 316-327. But I would like to see a more simple comparison of the different results. I find several issues: (a) line 320: (~ 20 ppbv) is not a ratio, and not clear how this compares to the MLS trends. (b) $\Delta(\text{ozone}) / \Delta(\text{NO}_y)$ from HALOE is about (1 ppmv / 2.6 ppbv); from ACE ~ 1 ppmv / 3 ppbv (Fig. 6b; the authors should include this), and from the model: 1 ppmv / 6 ppbv. These are close enough to be reasonably convincing, but this should be clearly spelled out (and discuss the factor of two difference from the model sensitivity, if I have done the algebra correctly).

Thanks very much for this set of comments, which led to numerous improvements in the manuscript. As the reviewer points out, the ACE relationships in Figure 6 can help as part of this discussion. This section was written somewhat sloppily in that we made use of HALOE NO_x measurements while in the model plots we showed NO_y. Because of the large diurnal variation of NO_x we have

eliminated NO_x from our discussion, and focus now exclusively on N₂O, NO_y, and O₃. We now have an extensive discussion comparing the N₂O, NO_y, and O₃ changes as observed by ACE, MLS, and the model, and provide some brief speculation and explanation concerning the differences between the measurements and the model. Essentially the entire text paragraph beginning with “The calculated equatorial N₂O changes ...” has been rewritten. In addition, this work led us to find an error in the modeling code was output to produce Figure 10 which resulted in a slight overestimate of NO_y. The middle panel of Figure 10 has been corrected to reflect this correction. This correction also improved the agreement in the absolute abundances between ACE and the model.

4) The authors make a convincing case of decreasing tropical stratospheric N₂O leading to ozone decreases, with a suggestion that this can result from decreasing tropical upwelling circulation. This is an especially interesting conclusion given the general result from model simulations of increasing trends in tropical upwelling (e.g. Butchart, *Rev. Geophys.*, 2014, and references therein). I think this conclusion should be discussed in more detail in regards to other recent work evaluating trends in stratospheric circulation, including: Engel et al (*Nat. Geo.*, 2009), Ray et al (*JGR*, 2010), Stiller et al (*ACP*, 2012), Diallo et al (*ACP*, 2012), Mahieu et al (*Nature*, 2014) and Ploeger et al (*JGR*, 2014).

While we certainly believe that our work does have implications for tropical upwelling, we are very hesitant to speculate too much on these implications given the relative simplicity of our 2D model calculations. We have, however, added two sentences at the end of Section 3.

“There is a burgeoning literature debating the possibility of changes in the stratospheric circulation [cf. Butchart, 2014 and references therein]. The results presented here may serve as a useful constraint for these analyses of long term stratospheric variability.”

1 **The Decrease in mid-Stratospheric Tropical Ozone Since**
2 **1991**

3

4

5

6 Gerald E. Nedoluha¹, David E. Siskind¹, Alyn Lambert², and Chris Boone³

7

8

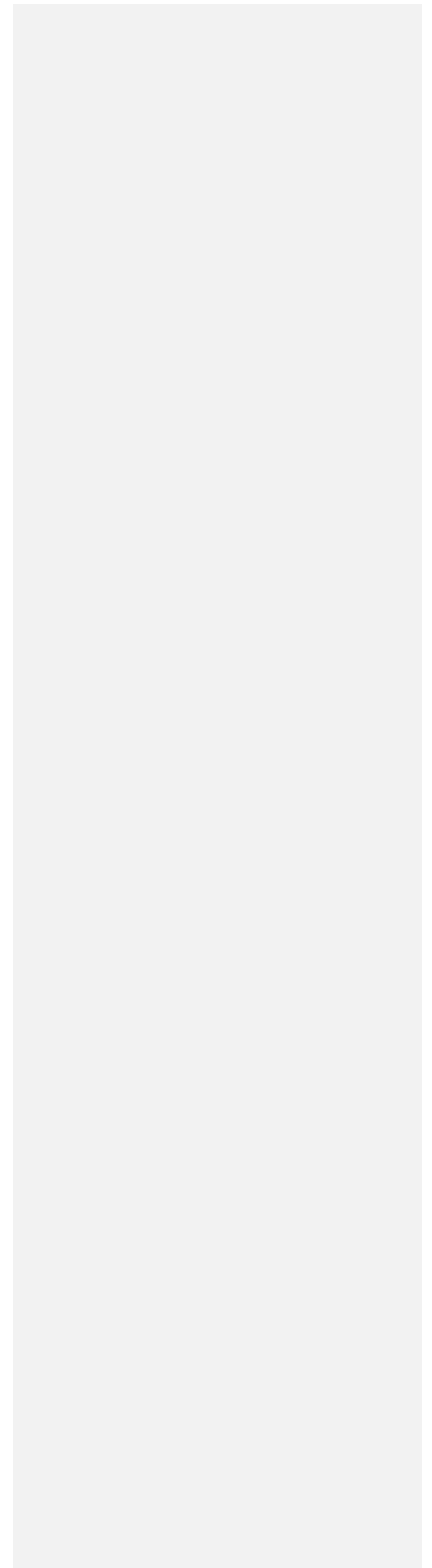
9

10 ¹Naval Research Laboratory, Washington, D. C., USA.

11 ²Jet Propulsion Laboratory, California Institute of Technology, Pasadena, California, USA

12 ³Department of Chemistry, University of Waterloo, Waterloo, Ontario, Canada.

13



14 **Abstract**

15 While global stratospheric O₃ has begun to recover, there are localized regions where O₃
16 has decreased since 1991. Specifically, we use measurements from the Halogen Occultation
17 Experiment (HALOE) for the period 1991-2005 and the NASA/Aura Microwave Limb Sounder
18 (MLS) for the period 2004-2013 to demonstrate a significant decrease in O₃ near ~10 hPa in the
19 tropics. O₃ in this region is very sensitive to variations in NO_y, and the observed decrease can be
20 understood as a spatially localized, yet long term increase in NO_y. In turn, using data from MLS
21 and from the Atmospheric Chemistry Experiment (ACE), we show that the NO_y variations are
22 caused by decreases in N₂O which are likely linked to long term variations in dynamics. To
23 illustrate how variations in dynamics can affect N₂O and O₃, we show that by decreasing the
24 upwelling in the tropics, more of the N₂O can photodissociate with a concomitant increase in
25 NO_y production (via N₂O+O(¹D) → 2NO) at 10 hPa. Ultimately, this can cause an O₃ decrease
26 of the observed magnitude.

27

28 **1. Introduction**

29 The slowdown in the O₃ decline and the beginnings of recovery of the ozone layer have
30 been documented [*Newchurch et al.*, 2003; *Yang et al.*, 2006]. Monitoring of the ozone layer
31 continues to be critical in order to understand ozone recovery as the CFC burden in the
32 stratosphere decreases. A number of observational studies have quantified the global distribution
33 of changes to the O₃ layer and revealed distinct patterns and variability which show that O₃
34 trends are not spatially uniform. One consistent result is that over decadal time scales, equatorial
35 O₃ in a vertical layer near 30 km (corresponding to ~10 hPa) often varies very differently from
36 O₃ in the rest of the middle to upper stratosphere. *Kyrolo et al.* [2013], using measurements from

37 the Stratospheric Aerosol and Gas Experiment (SAGE) from 1984-1997, show a general
38 decrease in O₃ which is statistically significant over much of the stratosphere, but an increase in
39 equatorial O₃ (albeit not statistically significant) in the 30-35 km region. Conversely, for the
40 period 1997-2011 *Kyrola et al.* [2013] show a general increase in O₃ from SAGE and Global
41 Ozone Monitoring by Occultation of Stars (GOMOS) measurements, but a statistically
42 significant decrease near 30 km in the tropics. [*Bourassa et al.* \[2014\] combine SAGE](#)
43 [measurements with measurements from the Optical Spectrograph and InfraRed Imager System](#)
44 [\(OSIRIS\) instrument and, again splitting the data into pre- and post-1997 periods, find very](#)
45 [similar results.](#) *Damadeo et al.* [2014] compute a SAGE trend from 1998-2005 and find a
46 [positive trend near 30km in the tropics and Northern Hemisphere, but a negative trend in the](#)
47 [Southern Hemisphere at this level.](#) Measurements from the Scanning Imaging Absorption
48 Spectrometer for Atmospheric Chartography (SCIAMACHY) instrument for the period 2002-
49 2012, reported by *Gebhardt et al.* [2014], show a pattern similar to the 1997-2011 pattern
50 reported by *Kyrola et al.* [2013], i.e. a strong statistically significant decrease in tropical O₃ in
51 the 30-35 km region while most of the middle atmosphere shows a slight increase in O₃.
52 Finally, *Eckert et al.* [2014] using Michelson Interferometer for Passive Atmospheric Sounding
53 (MIPAS) data from 2002-2012, also show a general increase in O₃ in most regions, but find
54 statistically significant negative trends in the tropics from ~25 hPa to 5 hPa. *Eckert et al.* [2014]
55 note that increased upwelling has been suggested as an explanation for ozone decreases, but, in
56 referring to these trends, they conclude that “upwelling does not provide a sufficient explanation
57 for the negative values in the tropical mid-stratosphere.”

58 Ozone at 10 hPa over the equator is particularly sensitive to catalytic cycles involving the
59 odd nitrogen (NO_x) chemical family [*Olsen et al.*, 2001; *Brasseur and Solomon*, 1986].

60 *Ravishankara* [2009] showed that N₂O would be the dominant ozone depleting substance emitted
61 in the 21st century, and pointed out that nitrogen oxides contribute most to O₃ depletion just
62 above where the O₃ mixing ratios are the largest. *Portmann et al.* [2012] calculated the effects of
63 a surface boundary increase of 20 ppbv of N₂O (an increase expected over ~20 years in the IPCC
64 A1B scenario) on O₃. They showed that this increase in N₂O emission would lead to a global
65 mean decrease of ~0.5-0.7% in O₃ just above the peak of the ozone mixing ratio (0.1 DU km⁻¹ in
66 the 30-35 km region where O₃ has a density of ~15-20 DU km⁻¹ based on their Figure 2). In
67 mixing ratio terms this gives a rate of ~5-7 ppbv/yr. *Plummer et al.* [2010] studied O₃ changes in
68 a model including GHGs and ODSs. They ran two experiments with a faster Brewer-Dobson
69 circulation, and these two experiments showed, at 10 hPa in the tropics, a decrease in reactive
70 nitrogen and an increase in both O₃ and N₂O at 10 hPa relative to the experiments with a slower
71 circulation. Thus variations in O₃ and N₂O at 10 hPa can be either correlated or anti-correlated
72 depending upon whether they are driven primarily by circulation or by changes in N₂O entering
73 the stratosphere.

Deleted: show an increase in global N₂O at 10 hPa from ~100 ppbv to 140 ppbv at 10 hPa from 1990-2010 while O₃ increases from ~8.2 ppmv to ~8.9 ppmv (~6 ppbv/yr). In their calculation the increases in residual

Deleted: result in

Deleted: in the mid to upper stratosphere

Deleted: specified increase in surface

74 In addition to long-term anthropogenically driven changes, events such as the eruption of
75 Mt. Pinatubo may alter the chemistry and dynamics of the stratosphere for extended periods.
76 *Aquila* [2013] compared a reference model with a model which simulated the effect of the
77 volcanic aerosols on both chemistry and dynamics. They calculated an increase in O₃ of ~2% at
78 10 hPa in the tropics slightly more than a year after the eruption, with no strong latitudinal
79 variation. *Damadeo et al.* [2014] attempt to disentangle anthropogenically driven changes from
80 Pinatubo eruption driven changes using an aerosol based volcanic proxy.

81 Previous observational work has correlated O₃ interannual variability in the tropics near
82 10 hPa with changes in specific odd nitrogen compounds; however, these studies were only for

91 relatively short time periods compared with the O₃ studies referenced above. *Randel et al.* [2000]
92 showed that the Halogen Occultation Experiment (HALOE) observed increasing NO+NO₂
93 coincident with decreasing O₃ from 1992-1997, but that these variations leveled-off during the
94 last years of HALOE measurements which were then available (1998-2000). The rate of O₃
95 decrease from 1992-1996 was faster than 100 ppbv/yr just above 10 hPa in the tropics. The
96 HALOE measurements of NO₂ at ~10 hPa from 1993-1997 were shown to be consistent with a
97 decrease in upward transport [*Nedoluha et al.*, 1998] and increased photolysis of N₂O, the source
98 of stratospheric NO_y.

99 The present study extends the previous observational studies with a combination of 21
100 years of ozone data from the UARS HALOE and the Aura Microwave Limb Sounder (MLS)
101 measurements, plus nitrogen species data from HALOE, MLS and the Atmospheric Chemistry
102 Experiment (ACE). Our results confirm the existence of the 10 hPa tropical ozone trend
103 anomaly and link it to a correspondingly consistent local change in the nitrogen species which
104 affect O₃. The resulting rate of change in O₃ and in the nitrogen species is an order-of-magnitude
105 faster than changes predicted from model calculations based upon changes in anthropogenic
106 emissions.

107

108 **2. Measurements from HALOE, Aura MLS, and ACE**

109 We make use of measurements from the HALOE, MLS, and the Fourier transform
110 spectrometer measurements from ACE. HALOE measurements of O₃, NO, and NO₂ are
111 available from 1991-2005. HALOE used the solar occultation technique which provided ~28-30
112 profiles per day in two latitude bands, one at sunrise and one at sunset. The latitude bands
113 drifted daily so that near global latitudinal coverage was provided in both sunrise and sunset

114 modes five times over the course of a year. The trends in the HALOE O₃ measurements have
115 been compared against SAGE II (*Nazaryan et al.*, 2005) and differences have been found to be
116 on the order of less than 0.3% per year in a majority of latitude bands at 25, 35, 45, and 55 km.

117 MLS measurements of O₃ and N₂O are available since 2004. MLS measurements are
118 available over a global range of latitudes on a daily basis. The stratospheric O₃ product has been
119 validated by *Froidevaux, et al.* [2008]. The N₂O measurements have been validated by *Lambert,*
120 *et al.* [2007].

121 Since 2004 ACE has been measuring O₃, N₂O, and the nitrogen species that constitute the
122 bulk of NO_y (NO, NO₂, HNO₃, and N₂O₅). As a solar occultation instrument it, like HALOE,
123 provides ~28-30 profiles per day in two latitude bands, one at sunrise and one at sunset. The
124 ACE O₃ measurements have been validated by *Dupuy et al.* [2009], and the NO and NO₂
125 measurements were validated by *Kerzenmacher et al.* [2008].

126

127 **2.1 The Solar Cycle and Linear Trend Calculations**

128 In cases where species are affected by the solar cycle, one of the challenges in
129 interpreting decadal scale trends in the stratosphere is separating these trends from solar cycle
130 induced variations. Model studies provide some guidance as to the expected solar cycle
131 variations in the species of interest. *Egorova et al.* [2005] used the SOCOL Chemistry Climate
132 Model (CCM) and found that at 30 km O₃ was higher at solar maximum when compared to solar
133 minimum, but that the difference was <3%. The N₂O mixing ratio at 30 km from 30°S-30°N was
134 found to be no more than 2% higher at solar minimum compared to solar maximum, and no more
135 4% from 30°N-60°N and 30°S-60°S. Schmidt et al. [2010] used the HAMMONIA general
136 circulation and chemistry model, and found an equatorial O₃ sensitivity of ~1.4+/-0.4%/100 solar

137 flux units (sfu), where the difference between the 1989 solar max and the 1986 solar min is 166
138 sfu. The study of *Remsberg and Lingenfelter* [2010] shows a 3% ozone maximum-minimum
139 response to the solar cycle at ~35 km (~7 hPa) from the SAGE II measurements, with results
140 from the HALOE measurements and from model calculations showing a smaller ozone response
141 to the solar cycle. As discussed in *Hood and Soukharev* [2006], NO_y in the upper stratosphere is
142 also affected by the solar cycle. They place an upper limit of ~10% on the solar cycle variations
143 in NO_y in the tropical mid-stratosphere. The model calculations in *Egorova et al.* [2005] show
144 an NO₂ solar cycle variation of <1%, and *Nedoluha et al.* [1998] show a similarly small variation
145 from the CHEM2D model (*Bacmeister et al.*,1998).

146 Throughout this study we will calculate trends based on a function including terms to fit
147 the annual, semi-annual, QBO, plus a constant term and a linear trend term. The QBO terms
148 were calculated using the Center for Climate Prediction 30 hPa and 50 hPa winds anomalies
149 obtained from www.cpc.ncep.noaa.gov/data/indices/. In addition to these terms we have
150 calculated trends from the HALOE measurements both with and without the inclusion of a solar
151 cycle term, where the solar cycle fit is calculated using the Mg II values obtained from the
152 [Laboratory for Atmospheric and Space Physics \(LASP\)](http://lasp.colorado.edu/lisird) Interactive Solar Irradiance Datacenter
153 at lasp.colorado.edu/lisird. We will only show HALOE trend calculations where a solar cycle
154 term has been included, but we have compared trends with and without the solar cycle term and
155 found that the results are similar.

156 The MLS measurement time series used here extends from 2004-2014, and therefore
157 clearly does not extend over a full solar cycle. The linear trend calculations from MLS
158 measurements which will be shown cover the period August 2004 to May 2013. Because Solar
159 Cycle 24 is particularly weak the Mg II values in 2013 are comparable to those in 2004, so solar

Deleted: Lasp

161 effects are unlikely to cause a trend in the MLS dataset used here. In order to provide an estimate
162 of the uncertainty in the trend which is introduced by the presence of a solar cycle we will show
163 some MLS results both with and without the inclusion of a solar cycle term. We will show that
164 in the region of greatest interest, near the tropics at ~10 hPa, the MLS trends appear to be nearly
165 insensitive to the presence of a solar cycle.

166

167 **2.2 Measurements of O₃, 1991-2014**

168 In Figure 1 we show the annual median O₃ anomalies from 5°S-5°N as measured by both
169 HALOE and Aura MLS at 10 hPa. This figure also shows that the O₃ decrease at 10 hPa has
170 occurred gradually over the period shown. There have been numerous studies combining O₃
171 timeseries from multiple satellites to derive long-term trends (e.g. *Jones et al.*, 2009; *Kyrola et*
172 *al.*, 2013), and there are several projects underway to provide long-term data records of
173 stratospheric composition, so we will not attempt here to produce a combined HALOE-MLS O₃
174 timeseries for trend calculations. The MLS timeseries anomalies shown have simply been offset
175 by a shift in mixing ratio so that the anomaly point for 2005 (which covers data taken during the
176 period July 2004 through June 2005) agrees with the HALOE anomaly at that point. The
177 anomalies are calculated by fitting annual and semi-annual cycles to each dataset separately and
178 then calculating annual median differences from this fit. The annual anomaly is sampled four
179 times per year so that each point represents an anomaly over either January-December, April-
180 March, July-June, or October-September. Each measurement is therefore included in four data
181 points in the figure. Having removed the annual cycle, the primary variation in O₃ in this region
182 is caused by the QBO. In addition to these QBO variations there is a clear decrease in O₃ over
183 the 21 years shown.

184 An estimate of the uncertainty in these annual medians can be obtained from the standard
185 deviation of the individual anomalies. The average value of $\sigma/n^{1/2}$ for the annual median
186 HALOE O₃ anomalies is 0.026 ppmv. The last annual anomaly has the largest uncertainty with
187 $\sigma/n^{1/2}=0.056$ ppmv. For the MLS, which has many more measurements, the largest annual
188 median uncertainty calculated by this method is 0.0027 ppmv.

189 In Figure 2 we show the linear trend in the global HALOE ozone measurements from
190 1991-2005. [Remsberg \[2008\] show a quite similar figure \(their Figure 13\) for linear trends in](#)
191 [HALOE O₃, but in %/decade. They found that the trends near 10 hPa from ~25°S to ~25°N had](#)
192 [a confidence interval of >90% for their partial tank order correlations \(Remsberg et al., 2001\).](#)
193 The trend is negative (i.e. O₃ is decreasing) near ~10 hPa with the most negative values
194 occurring in the tropics. Most of this study will focus primarily on the causes of this O₃ decrease
195 in this region. In general the results are very similar whether or not a solar cycle is included in
196 the fit, but the local tropical minimum at ~4 hPa does not appear when such a term is not
197 included.

198 HALOE measurements ceased in 2005, and Aura MLS has been providing O₃
199 measurements since 2004. In Figure 3 we show the linear trend in O₃ as measured by MLS.
200 MLS shows that the negative ozone trend in the tropics near ~10 hPa continued from August
201 2004 to June 2013. Inclusion of the most recent MLS data (from July 2013 to Sept. 2014) does
202 not result in a qualitative change in Figure 3, but does reduce the magnitude of the measured
203 trends. Again, the O₃ linear trends shown in Figure 3 have been calculated with a solar cycle
204 included in the fit, but the results are very similar with and without a solar cycle term. Several
205 other datasets have also shown decreasing O₃ near 10 hPa in the tropics. *Kyrola et al.* [2013] has
206 shown a decrease for 1997-2011 from SAGE and GOMOS, *Gebhardt et al.* [2014] for 2002-

207 2012 using measurements from SCIAMACHY, and *Eckert et al.* [2014] for 2002-2012 using
208 MIPAS measurements. There is some overlap between the negative HALOE O₃ trend (1991-
209 2005) and the positive SAGE O₃ trend shown by [*Kyrola et al.*, 2013] (1984-1997). Given the
210 excellent agreement between SAGE II and HALOE trends [e.g. *Nazaryan et al.*, 2005], and the
211 eruption of Mt. Pinatubo near the middle of the 1984-1997 timeseries, we expect this difference
212 between the 1984-1997 and 1991-2005 trends is caused by a real change in O₃ trends in the
213 tropical 10 hPa region in between 1991 and 1997.

214 While Figure 1 shows a general decrease in O₃ at 10 hPa over the entire HALOE
215 measurement period, and Figure 3 shows that this trend continued into the MLS measurements
216 period, such trends do not always persist over such extended periods. For example, away from
217 the tropics the 1991-2005 HALOE and 2004-2013 MLS trends near 10 hPa show clear,
218 hemispherically dependent, differences. Whereas the HALOE trends show a decrease in O₃ at
219 all latitudes near 10 hPa, the MLS trends show a sharp increase in O₃ at Southern mid-latitudes,
220 and a smaller decrease at similar pressure levels in Northern mid-latitudes.

221 Just as the HALOE and MLS trends show clear differences away from the tropics, they
222 also show clear differences in the tropics at other levels. The 1991-2005 HALOE trend shows an
223 increase in tropical O₃ near 30 hPa, but this is dominated by the strong increase from ~1991-
224 1999, followed by a period of stability in this region from 1999-2005. The MLS O₃
225 measurements suggest that this period of stability near 30 hPa continues through 2013. However
226 *Gebhardt et al.* [2014] do show statistically significant O₃ increases in the 2002-2012
227 SCIAMACHY measurements below 30 km with two local maxima, one near 22 km and one near
228 27 km, while *Eckert et al.* [2014] show an O₃ increase from 2002-2012 near 22 km (~50 hPa)
229 but a decrease near 27 km (~25 hPa) from the MIPAS measurements. In their 1984-1997 O₃

230 trends *Kyrola et al.* [2013] show an increase at 24 km, but a much larger decrease at 21 km.
231 Thus, while several measurements show decadal scale tropical trends near 10 hPa, such trends do
232 not appear to be common near 30 hPa, nor at other latitudes near 10 hPa.

233

234 **2.3 The Effect of Changes in Nitrogen Species on Ozone**

235 As noted above, O₃ in the tropical mid-stratosphere is particularly sensitive to changes in
236 NO_y which result from photodissociation and oxidation of N₂O [*Olsen et al.*, 2001], and long-
237 term *increases* in anthropogenic N₂O emission are expected to play a significant role in causing
238 future *decreases* in O₃ [*Portman et al.*, 2012]. However, N₂O is also a sensitive indicator of
239 upward transport and, as we show below, these variations in transport lead to a positive, not
240 negative correlation between N₂O and O₃. Figure 4 presents the correlation between MLS N₂O
241 and O₃ from 2004-2013. These correlations are calculated by first finding a zonal monthly
242 median for each year of MLS data and then subtracting from each of these the average MLS
243 monthly median for that month. Note the strongly positive correlation precisely where the
244 observed long term trends indicate ozone decreases. Figure 5 presents monthly median MLS
245 N₂O and O₃ data from 5°S-5°N at 10 hPa. The positive correlation between N₂O and O₃ is clearly
246 present on seasonal and interannual timescales and rules out an anthropogenic increase in N₂O as
247 the cause of the long term ozone decreases we observe.

248 This positive correlation between N₂O and O₃ in the tropical middle stratosphere can be
249 readily understood in the context of the relationship between N₂O, NO_y and O₃. This is
250 demonstrated in Figure 6 which presents ACE measurements of O₃, N₂O and the species which
251 make up the bulk of NO_y at 30 km (~10 hPa) from 10°S-10°N. While ACE does not provide the
252 daily measurement coverage in the tropics obtained by MLS, it does measure all of the species

253 relevant to the nitrogen chemistry which determines O₃ near ~10 hPa in the tropics. Like MLS,
254 ACE shows a strong positive correlation between N₂O and ozone. ACE also shows the expected
255 anticorrelation resulting from the chemistry of O₃ and NO_y. Figure 6c shows the anti-correlation
256 between NO_y and N₂O without which the correlation between N₂O and O₃ would not exist. This
257 anti-correlation of N₂O and NO_y can be understood as a coupled chemical/dynamical effect.
258 During periods when upward transport is slower, more N₂O at a given altitude is dissociated,
259 thus producing more NO_y at that altitude. We thus conclude that over the period of the MLS
260 measurements the effect of changes in transport on N₂O in this region on NO_y and hence O₃
261 dominate any increase in N₂O due to changing tropospheric emissions.

262 As indicated in Section 2.1, the MLS instrument has been operational for less than a full
263 solar cycle; hence for tropical trend calculations we show results both with and without the
264 inclusion of a solar cycle term. In Figure 7 we show the calculated profiles as a function of
265 pressure as derived from eight (constant term, two annual terms, two semi-annual terms, two
266 QBO terms, and a linear trend) and nine (including a solar cycle) parameter fits to the monthly
267 median MLS measurements. Figure 7 shows the profiles (the constant terms from the fits) in
268 addition to the linear trend and the net effect of 8 years of such a trend (2004-5 vs. 2012-13).
269 The O₃ trend results are in good agreement with those shown by *Gebhardt et al.* [2013] for
270 August 2004-April 2012, where the fastest decreasing trend in MLS O₃ is ~7%/decade.
271 *Gebhardt et al.* [2013] show that the MLS trends in O₃ are not statistically different from those
272 observed by SCIAMACHY or OSIRIS. While the inclusion of the solar cycle term fit clearly
273 does affect the linear trend at some levels, it does not alter the qualitative result that O₃ and N₂O
274 both show a statistically significant decrease over a similar range of pressures near 10 hPa. This

275 further reinforces the conclusion that this decrease in O₃ is caused by an increase in NO_y
276 (resulting from increased dissociation of N₂O) during this period.

277 As was shown in Figure 2, HALOE measurements showed a decrease in O₃ from 1992-
278 2005 at 10 hPa from 5°S-5°N. While HALOE did not provide measurements of N₂O, and did not
279 provide the full complement of NO_y species that is available from ACE, it did provide
280 measurements of two of the key odd-nitrogen species, NO and NO₂.

281 In Figure 8 we show annual median HALOE anomalies in O₃ alongside those of
282 NO+NO₂. Because NO+NO₂ has a strong diurnal component (unlike the set of NO_y
283 measurements provided by ACE), the anomalies for both species are calculated separately for
284 sunrise and sunset measurements. We have multiplied the sunset NO+NO₂ measurements by 0.4
285 so that they fit onto the same scale as the sunrise measurements. The average (maximum) $\sigma/n^{1/2}$
286 value for sunrise NO+NO₂ is 0.064 ppbv (0.082 ppbv), while for the sunset measurements
287 (before multiplication by 0.4) it is 0.122 ppbv (0.22 ppbv). For the O₃ sunrise measurements the
288 average (maximum) $\sigma/n^{1/2}$ value is 0.045 ppmv (0.064 ppmv), while for the sunset measurements
289 it is 0.049 ppmv (0.081 ppmv).

290 Figure 8 shows that NO+NO₂ generally was increasing over the course of the HALOE
291 measurements and that this increase tracked the ozone decrease, both on a year-to-year timescale
292 (dominated by the quasi-biennial oscillation, QBO) and over the full 1992-2005 time period.
293 There is a slight (~3-month) apparent phase-lag between the sunset and sunrise NO+NO₂
294 measurements from ~1998-2003 which is not apparent in the O₃ anomalies and for which we
295 have no explanation. With the exception of this feature, the general consistency between the
296 QBO driven variations in O₃ and NO+NO₂, and the trend which is apparent in both the O₃ and
297 NO+NO₂ measurements, provides added confidence that the decrease in O₃ and the increase in

298 NO+NO₂ measured by HALOE from 1992-2005 are both correct and, further, are coupled. As
299 we concluded from the MLS measurements from 2004-2013, this change suggests a slowdown in
300 upward transport in this region from 1992-2005. Note, this is consistent with the results of
301 *Nedoluha et al.* [1998] who interpreted the decreases in upper stratospheric CH₄ from 1992-1996
302 as linked with a simultaneous increase in NO₂ at 30 km. Our results here extend that early result
303 to encompass the entire 13 year UARS mission.

304 In Figure 9 we show the calculated linear trends in the HALOE O₃ and NO+NO₂
305 measurements. As in Figure 8 we separate the HALOE sunrise and sunset measurements, and
306 calculate trends for four separate measurements: sunrise and sunset O₃ and sunrise and sunset
307 NO+NO₂. Encouragingly, despite having very different vertical profiles, the shape of the sunrise
308 and sunset NO+NO₂ trend profiles are very similar. The O₃ sunrise and sunset trends also agree
309 well, and the pressure level of the minimum of the observed decrease in these O₃ measurements
310 corresponds closely with the maximum in the observed increase in the NO+NO₂ measurements.

311

312 3. Model Calculations

313 In order to better understand the changes in the observed species we have employed the
314 two-dimensional chemical transport model (CHEM2D) (*Bacmeister et al.*, 1998). The model
315 includes parameterized gravity wave and planetary wave drag and is ideal for understanding
316 tracer transport and the response of the global middle atmospheric circulation to external
317 forcings. Compared with those earlier studies, the present model has an improved vertical
318 resolution (1 km, instead of 2 km). CHEM2D's most recent applications have included
319 simulating the solar cycle variations of polar mesospheric clouds (*Siskind et al.*, 2005) and

Deleted: model's

Deleted: has been doubled to

Deleted: .

323 studying the response of stratospheric ozone to both the solar cycle and the tropical quasi-
324 biennial oscillation (*McCormack et al., 2007*)

325 We will show results from two model runs, each of which has been integrated for 12
326 years to ensure stability from year-to-year. Since the goal of the model was to test whether
327 dynamical changes would affect N₂O, NO_y, and O₃ at the equator, we introduced a very simple
328 perturbation. The two models differ only in that, in one case, we added a small heat source of
329 0.3 K/day, centered at 18 km at the equator, similar to Experiment 7 of *Bacmeister et al (1998)*.
330 In addition, we recognize that the model differences shown represent two equilibrium solutions
331 while the calculated trends show the effects of an atmosphere changing over time. Nonetheless,
332 a comparison of these two models can serve as an indication whether it is possible to reproduce
333 the observed changes in the measured species with a dynamical perturbation.

334 Figure 10 shows the change in N₂O, NO_y, and O₃ at the equator resulting from this
335 dynamical perturbation. The absolute values for these three species at 10 hPa are in very good
336 general agreement with those shown in Figure 6 from the ACE measurements. The N₂O
337 chemistry is relatively simple, and N₂O at all levels is lower for the case of the slower tropical
338 ascent which offers more time for dissociation. At 10 hPa the case with the slower ascent shows
339 ~22 ppbv less N₂O. Unlike the measurements, however, the N₂O in the model changes over a
340 deep layer, covering the entire pressure range from 50-1hPa.

341 The calculated equatorial N₂O changes shown in Figure 10 correspond with calculated O₃
342 and NO_y profile changes which are in the same sense and general magnitude as the observations.
343 Thus the calculation with lower N₂O yields increased NO_y due to increased oxidation. via
344 N₂O+O(1D) -> 2NO; the baseline model with ~22 ppbv less N₂O shows an increase of ~1.3
345 ppbv in NO_y, so ΔNO_y/ΔN₂O ~0.065. This is similar to the ΔNO_y/ΔN₂O in the ACE

Deleted: 20

Deleted: Figure 10 also shows the calculated O₃ and NO_y profile changes at the equator for the same two model runs. Between 5-15 hPa and including the peak of the layer, the baseline model with less heating shows ~0.3 ppmv less O₃, and the total NO_y is higher. The increase NO_y results from increased photodissociation of N₂O via N₂O+O(1D) -> 2NO. The ratio of the O₃ and N₂O changes (~20 ppbv) in the model are qualitatively similar to the trends in the MLS observations near ~10 hPa (~0.1 ppmv/yr for O₃, ~4 ppbv/yr for N₂O). Similarly, we can qualitatively compare the HALOE O₃ and NO_x differences in the two model runs. The largest decrease in HALOE O₃ is ~0.06 ppmv/yr, which is accompanied by a sunset NO_x trend of ~0.16 ppbv/yr. The ratios of measured O₃ change relative to NO_x change is qualitatively similar to the ratio of the model change in O₃ (~0.3 ppmv) to the model change in NO_x (~1.9 ppbv). The qualitative agreement between models and both the HALOE

Formatted: Don't keep with next

367 measurements in Figure 6c, which is ~.075. Regarding ozone, the baseline model with less
368 heating and 1.3 ppbv greater NO_y shows about ~0.26 ppmv less O₃ at 10 hPa. This yields a
369 ΔO₃/ΔNO_y of ~200 which is on the order of, but somewhat less than, the observed ΔO₃/ΔNO_y
370 from the ACE measurements (which is closer to ~330). We can also directly compare the
371 calculated quantity ΔO₃/ΔN₂O in the model and in the ACE and MLS measurements; here we
372 also get a somewhat reduced ozone response compared with the observations. Whereas the
373 model shows a ΔO₃/ΔN₂O of ~12, ACE and MLS both show ΔO₃/ΔN₂O ~25). About 25% of
374 this difference is because the model ΔNO_y/ΔN₂O sensitivity is slightly less than observed. Also,
375 since our approach towards diurnal averaging requires a specific of a single night-to-day ratio
376 (cf. *Summers et al.*, 1996) it is possible that we are underestimating the diurnally averaged
377 response of O₃ to NO_x chemistry, which varies strongly with the time of day. Nevertheless, the
378 qualitative agreement between the model and the ACE and MLS measurements supports the idea
379 that the observed O₃ change can be caused by a dynamical perturbation.

380 While the model runs do support the suggestion that the changes in O₃ and N₂O observed
381 near the equator at ~10 hPa can be caused by a dynamical perturbation, we do note that this
382 particular dynamical perturbation also shows large differences in other regions where the
383 measured trends are small and/or vary in a temporally different manner than do the tropical 10
384 hPa measurements. No doubt a number of dynamical changes affected N₂O over the period
385 1991-2013, and these variations drove changes in NO_x and in turn O₃. What we conclude here is
386 that, because of changes in transport, the N₂O which arrived in this region experienced
387 significantly more dissociation in 2013 than in 2004, and, based on inferences from the HALOE
388 O₃ and NO_x measurements, that this trend was also present throughout much of the HALOE
389 measurement period. We note that there is a burgeoning literature debating the possibility of

390 [changes in the stratospheric circulation \[cf. Butchart, 2014 and references therein\]. The results](#)
391 [presented here may serve as a useful constraint for these analyses of long term stratospheric](#)
392 [variability.](#)

393

394 **4. Summary**

395 Ozone measurements from HALOE and MLS show a long-term decrease in O₃ in the
396 tropical mid-stratosphere near the peak of the O₃ mixing ratio. O₃ in this region is very sensitive
397 to variations in NO_y, and the observed decrease in O₃ can be understood in terms of the effects of
398 increasing NO_y. From MLS and ACE measurements we conclude that the NO_y variations are the
399 result of a decrease in N₂O from 1992-2012 resulting from changes in the dynamics over this
400 period. Using a 2D model, we show that a perturbation of the dynamics results in changes in
401 N₂O, NO_y, and O₃ which are qualitatively consistent with the observed trends. [In future it would](#)
402 [be interesting to study N₂O, NO_y, and O₃ variations in this region in more sophisticated 3D](#)
403 [models.](#)

404 A feature of particular interest for future work is the increase in O₃ observed in the
405 Southern Hemisphere mid-stratosphere by MLS. Both the overall increase in O₃ in this region as
406 well as the short-timescale variations are well correlated with changes in N₂O, suggesting that
407 this O₃ variation is also dynamically controlled.

408

409 **Acknowledgments.** This project was funded by NASA under the Upper Atmosphere Research
410 Program, by the Naval Research Laboratory, and by the Office of Naval Research. Work at the
411 Jet Propulsion Laboratory, California Institute of Technology, was carried out under a contract
412 with the National Aeronautics and Space Administration. MLS and HALOE data are available

413 from the NASA Goddard Earth Science Data Information and Services Center
414 (acdisc.gsfc.nasa.gov). ACE-FTS data is available at www.ace.uwaterloo.ca.

415

416 **References**

417 Aquila, V., et al, The Response of Ozone and Nitrogen Dioxide to the Eruption of Mt. Pinatubo
418 at Southern and Northern Midlatitudes (2013), *J. Atmos. Sci.*, 70, 894-900.

419 Bacmeister, J. T., D. E. Siskind, M. E. Summers, and S. D. Eckermann, (1998) Age of air in a
420 zonally averaged two-dimensional model, *J. Geophys. Res.*, 103, D10, 11263-11288.

421 [Bourassa, A E., D. A. Degenstein, W. J. Randel, J. M. Zawodny, E. Kyrola, C. A. McLinden, C.
422 E. Sioris, and C. Z. Roth \(2014\), Trends in stratospheric ozone derived from merged SAGE II
423 and Odin-OSIRIS satellite observations, *Atmos. Chem. Phys.*, 14, 6983–6994, 2014.](#)

424 Brasseur, G. P. and S. Solomon (1986), *Aeronomy of the Middle Atmosphere*, D.Reidel press.

425 [Butchart, N., The Brewer-Dobson circulation \(2014\), *Rev. Geophys.*, 52, 157–184,
426 doi:10.1002/2013RG000448.](#)

427 [Damadeo, R. P., J. M. Zawodny, and L. W. Thompson \(2014\), Reevaluation of stratospheric
428 ozone trends from SAGE II data using a simultaneous temporal and spatial analysis, *Atmos.
429 Chem. Phys.*, 14, 13455–13470, 2014.](#)

430 Dupuy, E., et al. (2009), Validation of ozone measurements from the Atmospheric Chemistry
431 Experiment (ACE), *Atmos. Chem. Phys.*, 9, 287–343, 2009.

432 Eckert, E., et al. (2014), Drift-corrected trends and periodic variations in MIPAS IMK/IAA
433 ozone measurements, *Atmos. Chem. Phys.*, 14, 2571–2589, 2014.

434 Egorova, T., et al. (2005), Influence of solar 11-year variability on chemical composition of the
435 stratosphere and mesosphere simulated with a chemistry-climate model, *Advances in Space
436 Research* 35 (2005) 451–457.

437 Froidevaux, L., et al. (2008), Validation of Aura Microwave Limb Sounder stratospheric ozone
438 measurements, *J. Geophys. Res.*, 113, D15S20, doi:10.1029/2007JD008771.

439 Gebhardt, C., et al. (2014), Stratospheric ozone trends and variability as seen by SCIAMACHY
440 during the last decade, *Atmos. Chem. Phys.*, 14, 831–846, 2014.

441 Jones, A., et al., (2009), Evolution of stratospheric ozone and water vapour time series studied
442 with satellite measurements, *Atmos. Chem. Phys.*, 9, 6055–6075, 2009.

443 Kerzenmacher, T., et al. (2008), Validation of NO₂ and NO from the Atmospheric Chemistry
444 Experiment (ACE), *Atmos. Chem. Phys.*, 8, 5801–5841, 2008.

445 Kyrola, E., et al. (2013), Combined SAGE II–GOMOS ozone profile data set for 1984–2011 and
446 trend analysis of the vertical distribution of ozone, *Atmos. Chem. Phys.*, 13, 10645–10658,
447 2013

448 Lambert, A., et al. (2007), Validation of the Aura Microwave Limb Sounder middle atmosphere
449 water vapor and nitrous oxide measurements, *J. Geophys. Res.*, 112, D24S36,
450 doi:10.1029/2007JD008724

451 McCormack, J. P. D. E. Siskind, and L. L. Hood, Solar-QBO interaction and its impact on
452 stratospheric ozone in a zonally averaged photochemical transport model of the middle
453 atmosphere (2007) *J. Geophys. Res.*, 112, D16109, doi:10.1029JD008369.

454 Nazaryan, H., M. P. McCormick, and J. M. Russell III (2005), New studies of SAGE II and
455 HALOE ozone profile and long-term change comparisons, *J. Geophys. Res.*, 110, D09305,
456 doi:10.1029/2004JD005425.

457 Nedoluha, G. E., et al. (1998), Changes in upper stratospheric CH₄ and NO₂ as measured by
458 HALOE and implications for changes in transport, *Geophys. Res. Lett.*, 25, 987–990.

459 Newchurch, M. J., Yang, E.-S., Cunnold, D. M., Reinsel, G. C., Zawodny, J. M., and Russell III,
460 J. M.: Evidence for slowdown in stratospheric ozone loss: first stage of ozone recovery (2003),
461 J. Geophys. Res., 108, 4507, doi:10.1029/2003JD003471, 2003.

462 Olsen, S. C., C. A. McLinden, and M. J. Prather, (2001) Stratospheric N₂O-NO_y system: Testing
463 uncertainties in a three-dimensional framework, J. Geophys. Res., 106, D22, 28771-28784

464 Plummer, D. A., et al. (2010), Quantifying the contributions to stratospheric ozone changes from
465 ozone depleting substances and greenhouse gases, Atmos. Chem. Phys., 10, 8803–8820, 2010.

466 Portmann, R. W., J. S. Daniel, and A. R. Ravishankara (2012), Stratospheric ozone depletion due
467 to nitrous oxide: influences of other gases, Phil. Trans. R. Soc. B (2012) 367, 1256–1264
468 doi:10.1098/rstb.2011.0377

469 Randel, W. J., et al. (2000), Interannual changes in stratospheric constituents and global
470 circulation derived from satellite data, in Atmospheric Science Across the Stratopause,
471 Geophys. Monogr. Ser., vol. 123, pp. 271– 285, AGU, Washington, D. C., 2000.

472 Ravishankara, A. R., et al., (2009), Nitrous Oxide (N₂O): The dominant ozone-depleting
473 substance emitted in the 21st century, Science 326, 123, DOI: 10.1126/science.1176985

474 Remsberg, E. [E., P. P. Bhatt, and L. E. Deaver \(2001\), Ozone changes in the lower stratosphere](#)
475 [from the halogen occultation experiment for 1991 through 1999, J. Geophys. Res., 106, 1639 –](#)
476 [1653, doi:10.1029/2000JD900596.](#)

477 [Remsberg, E. E. \(2008\), On the response of Halogen Occultation Experiment \(HALOE\)](#)
478 [stratospheric ozone and temperature to the 11-year solar cycle forcing, J. Geophys. Res., 113,](#)
479 [D22304, doi:10.1029/2008JD010189.](#)

480 [Remsberg, E.](#) and G. Lengenfelder (2010), Analysis of SAGE II ozone of the middle and upper
481 stratosphere for its response to a decadal-scale forcing, *Atmos. Chem. Phys.*, 10, 11779–
482 11790, 2010.

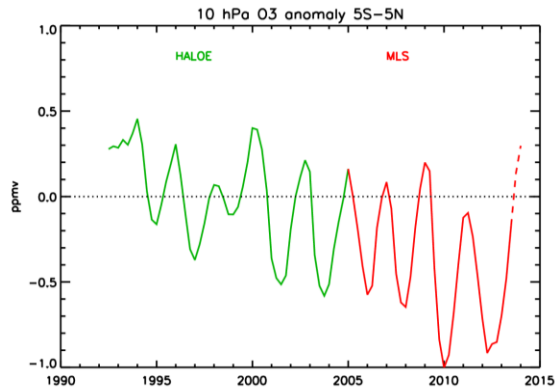
483 Schmidt, H., G. P. Brasseur, and M. A. Giorgetta (2010), Solar cycle signal in a general
484 circulation and chemistry model with internally generated quasi-biennial oscillation, *J.*
485 *Geophys. Res.*, 115, D00I14, doi:10.1029/2009JD012542.

486 Siskind, D. E., M. H. Stevens and C. R. Englert (2005) A model study of global variability in
487 mesospheric cloudiness, *J. Atm Solar Terr Phys.*, 67, 501-513.

488 [Summers, M. E., D. E. Siskind, J. T. Bacmeister, R. R. Conway, S. E. Zasadil, and D. F. Strobel,](#)
489 [\(1997\) Seasonal variation of middle atmospheric CH₄ and H₂O with a new chemical-](#)
490 [dynamical model. *J. Geophys. Res.*, 102, D3, 3503-3526.](#)

491 Yang, E.-S., Cunnold, D. M., Salawitch, R. J., McCormick, M. P., Russell III, J. M., Zawodny, J.
492 M., Oltmans, S., and Newchurch, M. J. (2006): Attribution of recovery in lower stratospheric
493 ozone, *J. Geophys. Res.*, 111, D17309, doi:10.1029/2005JD006371, 2006.

494

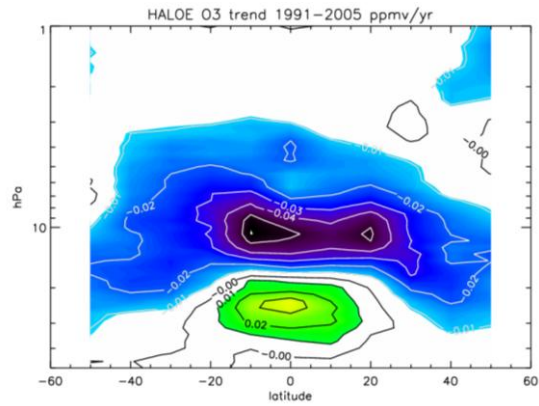


495

496 **Figure 1 - Annual median ozone anomalies at 10 hPa 5°S-5°N from HALOE (green; HALOE data is actually**
 497 **shown on its native grid at 30 km, which is ~10 hPa) and MLS (red). Annual anomalies are shown four times**
 498 **per year; hence each measurement is included in four datapoints. The MLS anomalies have been shifted by a**
 499 **constant mixing ratio so that the HALOE and MLS annual anomalies for 2005 (covering the period July**
 500 **2004-June 2005) agree. The MLS data from July 2013 onwards is indicated dashed in order to indicate that**
 501 **this data will not be used in any of the linear trend calculations to be shown.**

502

503



504

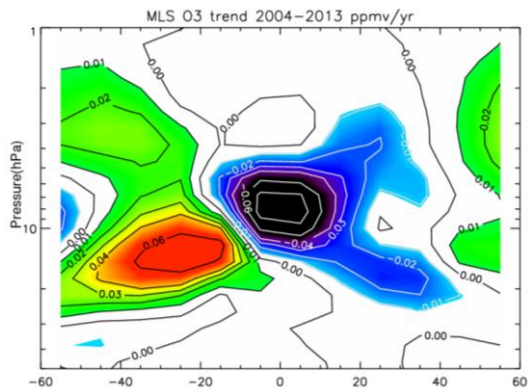
505 **Figure 2 - The calculated linear trend in HALOE ozone for 1991-2005. The HALOE data has been sorted**
506 **into eleven 10° latitude bins from 55°S to 55°N. Regions where the magnitude of the trend is <0.01 ppmv/year**
507 **are indicated in white.**

508

Formatted: Superscript

509

510



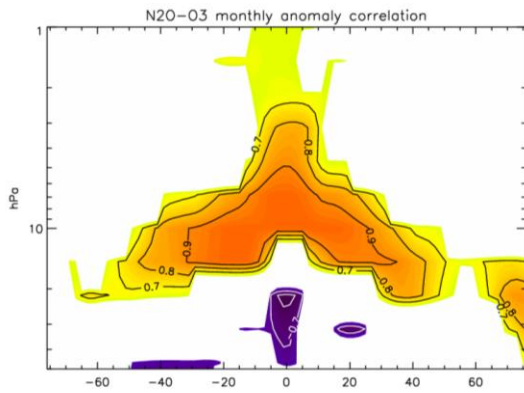
511

512 | **Figure 3 – The O_3 linear trend calculated from MLS data from August 2004- May 2013. Contour lines are**
513 **shown at +/-0.01, 0.02, 0.03, 0.04, 0.06, 0.08 ppmv/yr. The MLS data has been sorted into twelve 10° latitude**
514 **bins from 60° S to 60° N. Regions where the magnitude of the trend is <0.01 ppmv/year are indicated in white.**

515

Formatted: Subscript

516



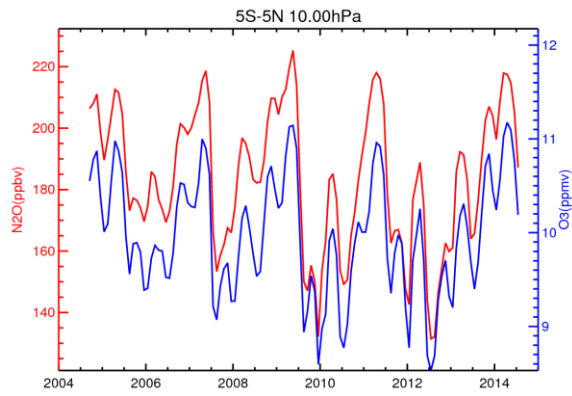
517
518

519 **Figure 4 – Correlation coefficients between N₂O and O₃ calculated from monthly median anomalies from**
520 **MLS data as a function of latitude and pressure. Results are shown for regions where the correlation (or**
521 **anti-correlation) is >0.6.**

522

523
524

525

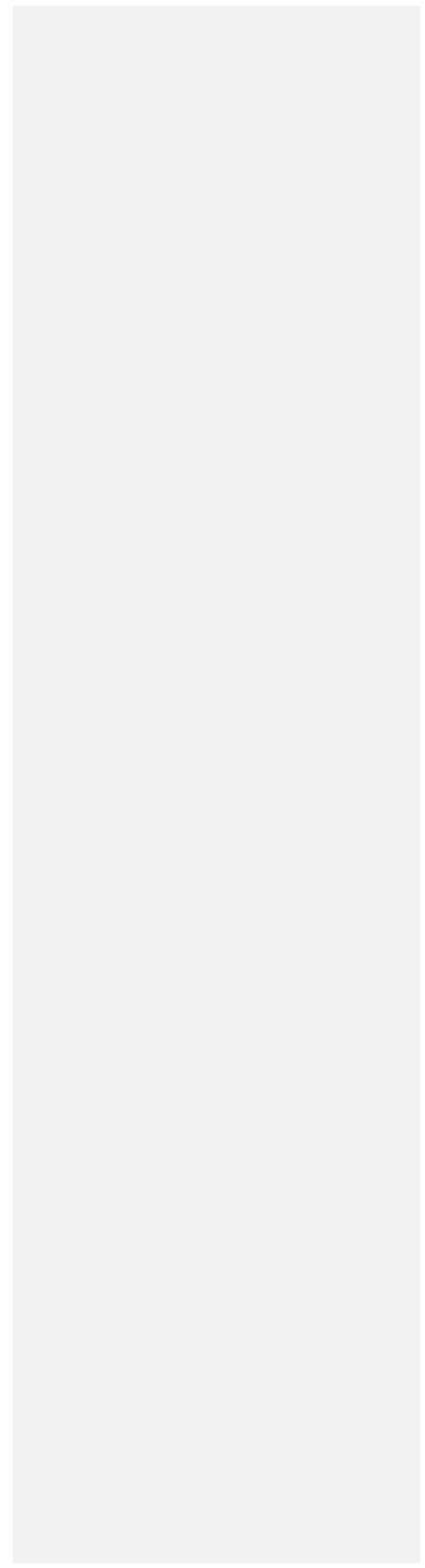


526

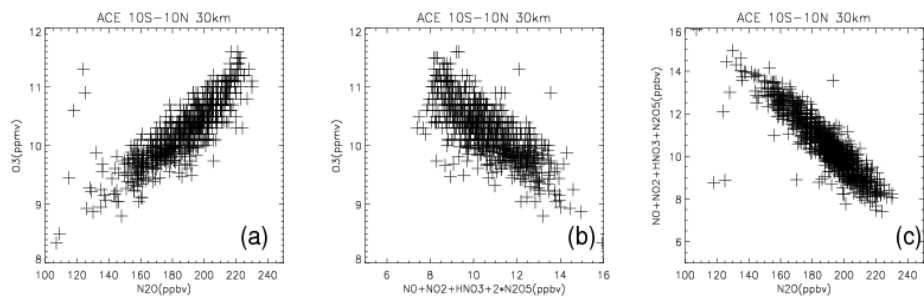
527 **Figure 5 – Monthly median N₂O (red) and O₃ (blue) mixing ratios at 10 hPa from MLS measurements**
528 **between 5°S and 5°N.**

529

530



531

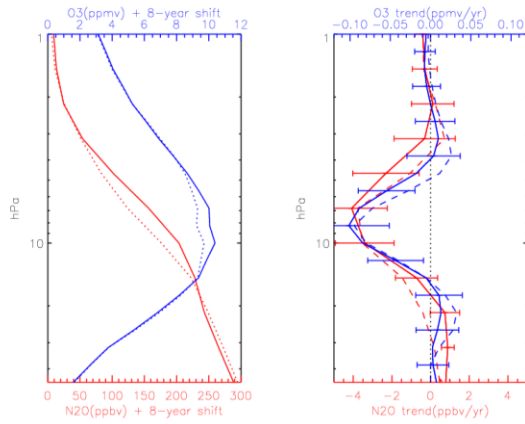


532

533 **Figure 6 – ACE measurements of O₃, N₂O, and the key members of the NO_y family,**
534 **NO+NO₂+HNO₃+2*N₂O₅. Measurements are shown for 10°S-10°N at 30 km. Both sunrise and sunset**
535 **measurements are included.**

536

537

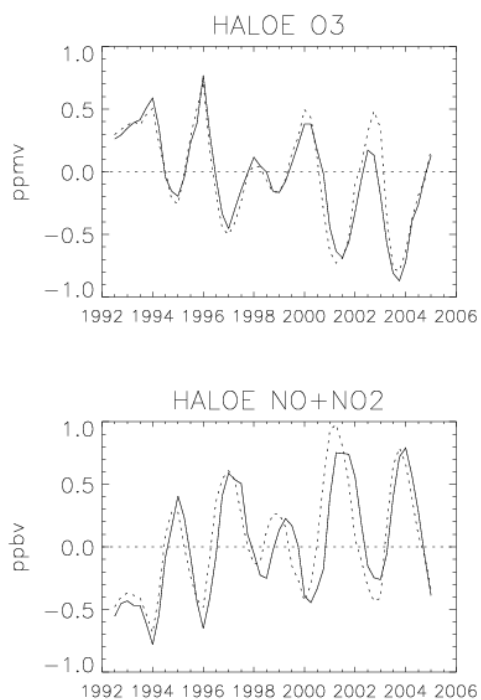


539

540 **Figure 7 - Left hand panel: Annual average MLS profiles of O₃ (blue; top scale) and N₂O (red; bottom scale)**
 541 **from 5°S-5°N. Shown are the constant term derived from the fit to the August 2004- May 2013 MLS**
 542 **measurements (solid), and the same term with an added 8-year shift (thus approximating the difference**
 543 **between the 2004/5 and 2012/13 MLS annual average) based on the linear trend applied over a period**
 544 **comparable to the length of the MLS dataset (dotted). Right hand panel: Linear annual trend calculated with**
 545 **a solar cycle term included (solid) and without a solar cycle term (dashed). Error bars (2σ) are similar for**
 546 **fits with and without the solar cycle, and are shown only for the former.**

547

548



549

550 **Figure 8 - Annual median HALOE O₃ (top) and NO+NO₂ (bottom) anomalies at 10 hPa from 5°S-5°N.**

551 **Annual anomalies are shown four times per year, hence each measurement is included in four datapoints.**

552 **Results are shown separately for sunrise (solid) and sunset (dashed). Sunset NO+NO₂ anomalies have been**

553 **multiplied by 0.4 so that they fit on the same scale as the sunrise anomalies.**

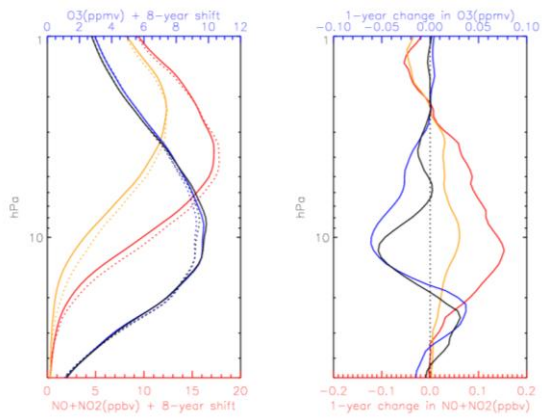
554

555

556

557

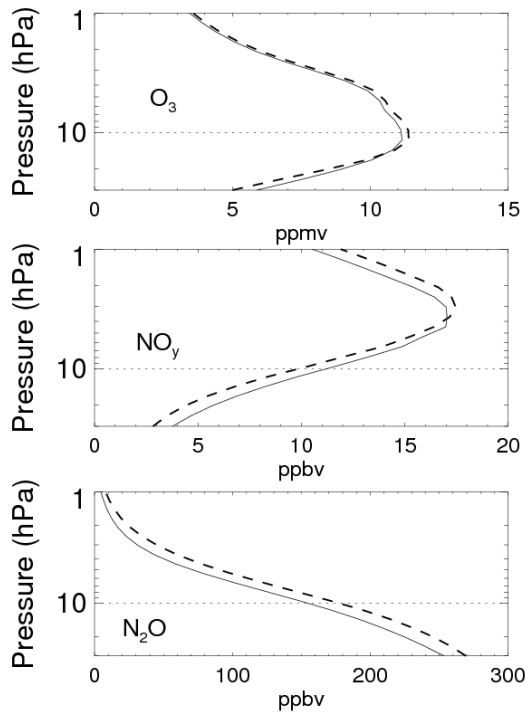
558



559
560

561 **Figure 9 - Left hand panel: Annual average HALOE profiles of O₃ at local sunset (blue; top scale), local**
 562 **sunrise (black; top scale) and NO+NO₂ at local sunset (red; bottom scale), and local sunrise (orange; bottom**
 563 **scale) from 5°S-5°N. Results are shown for the first year of HALOE measurements (solid) and with an 8-year**
 564 **shift (to allow for comparison with Figure 7) using the annual average trend shown on the right-hand panel**
 565 **(dashed). Right hand panel: 1-year changes based on linear trends over 5°S-5°N calculated from 1991-2005.**
 566 **Line colors are the same as in the left-hand panel.**

567



569

570

571 **Figure 10 - Annual average altitude profiles of O₃, NO_y, and N₂O for the equator. The solid curve is a**
572 **baseline run, while the dashed curve is a simulation which includes an additional 0.3 K/day heat source in the**
573 **lowermost stratosphere which acts to increase the tropical upwelling.**

574

575

